

# Structure and Properties of Polypropylene-Wrapped Carbon Nanotubes Composite

Wen-Hua Li,<sup>1,2</sup> Xiao-Hua Chen,<sup>2</sup> Zhi Yang,<sup>2</sup> Long-Shan Xu<sup>2</sup>

<sup>1</sup>College of Physics and Optoelectric Engineering, Guangdong University of Technology, Guangzhou 510006, China

<sup>2</sup>College of Materials Science and Engineering, Hunan University, Changsha 410082, China

Received 29 March 2007; accepted 10 January 2009

DOI 10.1002/app.30204

Published online 21 May 2009 in Wiley InterScience (www.interscience.wiley.com).

**ABSTRACT:** By means of *in situ* graft method, polypropylene (PP)-wrapped carbon nanotubes (CNTs) composite were prepared. Infrared spectroscopy (IR) results showed that there was covalent linkage between PP and CNTs via maleic anhydride (MAH) grafting. Owing to the uniform dispersion of CNTs and covalent adhesion between PP and CNTs, the tensile strength of PP-wrapped CNTs composite was higher than that for neat PP by 110%, and a 74% increase as compared to the CNTs/PP (with the same CNTs content) composite. The further test showed a strong mechanical behavior with up to 113% increase in

Young's modulus of the neat PP. Based on the uniform dispersion of CNTs, the electrical conductivity of PP-wrapped CNTs composite increased sharply by up to seven orders of magnitude with 4 wt % CNT fillers. As a result, the volume resistivity was decreased with increase in the CNT content that could be governed in a percolation-like power law with a relatively low percolation threshold. © 2009 Wiley Periodicals, Inc. *J Appl Polym Sci* 113: 3809–3814, 2009

**Key words:** carbon nanotubes; polypropylene; maleic acid anhydride

## INTRODUCTION

Because of the unique structural, mechanical, and electronic properties (metallic conductivity, chemical and thermal stability, extremely high elasticity, tensile strength, etc.) of carbon nanotubes (abbreviated as CNTs hereafter), many researchers have been trying to expand the utility of CNTs, especially to develop CNT-reinforced composites. Polymer composites reinforced with CNTs<sup>1–16</sup> are considered to have many engineering potentials, ranging from battery electrodes and electronic devices to much stronger composites. However, because of the atomically smooth surface of CNT, lack of interfacial bonding limits load transfer from the matrix to the CNT. Furthermore, with intrinsic van der Waals forces, nanotubes are typically held together as bundles and have very low solubility in most solvents. When mixed into polymer, nanotubes tend to exist as entangled agglomerates, and homogeneous dis-

persions are not easily obtained. Therefore, the strong interfacial bonding between nanotubes and polymer and the homogenous dispersion of CNTs in the polymer are necessary conditions to take full advantage of the extraordinary properties of CNTs for reinforcement of composites.

To gain polymer/CNTs composites with perfect performance, several approaches have been carried out. Polymer wrapped CNTs is an effective method. Curran<sup>17</sup> prepared poly (*m*-phenylenevinylene-*co*-2,5-dioctoxy-*p*-phenylenevinylene) (PmPV) wrapped CNTs composites in which the dispersion of the nanotubes was quite uniform, PmPV and CNTs had excellent interfacial wetting. The incorporation of CNTs made the composites a dramatic increase in conductivity by a factor of 10<sup>8</sup> for lower concentration of CNTs. O'Connell<sup>18</sup> prepared polyvinyl pyrrolidone (PVP) wrapped CNTs composites and polystyrene sulfonate (PSS) wrapped CNTs composites, wherein the polymer disrupted the hydrophobic interface with water and the smooth tube-tube interactions in aggregates. These solubilization composites open the door to the biological system for CNTs. Tang<sup>19</sup> prepared polyphenylacetylenes (PPAs) wrapped CNTs composites which are soluble in common organic solvents. The nanotubes dramatically stabilize the PPA chains against the harsh laser irradiation. The NT/PPAs found an array of potential applications in optics-related, especially laser-based, technologies.

Correspondence to: X.-H. Chen (liwenhuat@yahoo.com.cn).

Contract grant sponsor: National Natural Science Foundation of China; contract grant numbers: 50372020, 59972031.

Contract grant sponsor: Provincial Natural Science Foundation of Hunan, China; contract grant number: 01JJY2052.

*Journal of Applied Polymer Science*, Vol. 113, 3809–3814 (2009)  
© 2009 Wiley Periodicals, Inc.

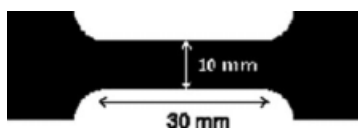


**Figure 1** The pattern of CNTs-MAH-PP composite for testing.

Polypropylene (PP) is widely used in many industrial applications because of its low cost and easy processing. CNT-reinforced PP systems hold the promise of delivering superior composite materials with high strength, light weight, and multifunctional features. Several studies are now being conducted on CNT-reinforced PP composite.<sup>9,10</sup> However, PP-wrapped CNTs composite have never been fabricated up to now. On one hand, PP, unlike PPAs or PSS in the examples, does not dissolve in water or organic solvent. On the other hand, it is well known that PP, as a consequence of its nonpolarity and crystallizability, exhibits very poor compatibility and adhesion toward other materials such as polymers, metals, and inorganic fillers. In this work, we developed a novel fabrication process for PP-wrapped CNT composites. In the preparation process of PP-wrapped CNTs, two steps have been taken. First, the maleic anhydride (MAH) was pretreated with CNTs which has been treated by sodium hydroxide (NaOH). In this step, the anhydride functions on MAH reacted with the hydroxyl group on the CNTs to form an ester group. Second, the MAH in CNTs-MAH was grafted onto PP upon the addition of benzoyl peroxide (BPO) when the CNTs-MAH was mixed with the molten PP.<sup>20</sup> The MAH acts as "bridge" function to bond both PP and CNTs by chemical reaction. This strong interfacial bonding between PP and CNTs by MAH grafting is beneficial for load-transfer processes between nanotubes and matrix.

## EXPERIMENTAL

CNTs in this study were fabricated by the chemical vapor deposition process in a furnace with a Ni-catalyst, where acetylene was used as a carbon source at temperature 700°C. The crude CNTs were stirred in 3 mol/L nitric acid and refluxed for 24 h at 60°C, and then suspended in 5 mol/L HCl solution for 6 h at 120°C. Subsequently the products were washed with distilled water many times until the pH value of the CNT solution reached 7, and then dried at 120°C.

A typical synthesis routine of CNTs-OH is as follows: 100 mL absolute alcohol solution containing purified CNTs (0.1 g) was sonicated at room temperature for about 2 h to disperse the CNTs. A 100 mL absolute alcohol solution containing NaOH (0.4 g)

was slowly added dropwise into the above CNT suspension solution with constant sonication at a reaction temperature of 80°C. The reaction mixture was sonicated for an additional 2 h at 80°C, after which the CNT solution was filtered and rinsed with absolute alcohol until the pH value of the CNT solution reached 7, and then dried at 60°C. The obtained black powder was collected as CNTs-OH.

CNTs-MAH was fabricated by an ultrasonic solution process. Typically, to a 200 mL round-bottom flask, CNTs-OH were dissolved in 80 mL ethyl acetate and sonicated. In another flask, 40 mL ethyl acetate, MAH were added and sonicated for 30 min. The MAH solution was added to the CNTs suspension dropwise under sonication. The mixture was then sonicated for another 3 h. The accelerating agent, perchloric acid, was added to the mixture. The resulting dispersion was decanted into a glass dish and allowed to stand at room temperature for 2 days. The products were further vacuum-dried at 60°C for 2 days to remove the residual solvents.

For the fabrication of PP-wrapped CNTs composite, we developed the following procedure. First, isotactic PP was dissolved in xylene at 135°C using an oil bath. The CNTs-MAH was dispersed in xylene and sonicated for 30 min. Second, both PP solution and CNTs-MAH suspension were mixed while stirring at 180 rpm. After 30 min, BPO was added into the mixture. The mixture including BPO was stirred for another 3 h at a temperature of 135°C. Finally, the mixture was cooled to 70°C and then was washed by acetone several times. The residual was dried for 24 h in a vacuum oven at 70°C. The obtained dried residual was PP-wrapped CNTs composite (abbreviated as CNTs-MAH-PP hereafter). All experiments were accomplished under nitrogen atmosphere. For comparison, CNTs/PP<sup>21</sup> composite (with same CNTs content) was prepared via melt mixing of CNTs with PP at 135°C.

The PP-wrapped CNTs composite were pressed by using a hot press at 215°C, 3 MPa into film of dumbbell plates about 2 mm in the thickness as shown in Figure 1. So was done for the CNTs/PP composite.

Infrared spectroscopy (IR) spectra of CNTs-OH, CNTs-MAH, PP, and PP-wrapped CNT composite in KBr pellets were performed on a 300E JASCO Fourier transform infrared spectrometer. The spectra were collected from 4000 cm<sup>-1</sup> to 600 cm<sup>-1</sup>, with a 4 cm<sup>-1</sup> resolution over 20 scans. Thermogravimetric measurements (TGA) were performed on a TA Instrument NETZSCH STA 449C at a heating rate of 10°C/min from 50°C to 600°C under nitrogen atmosphere. Morphology of CNTs and PP-wrapped CNTs composite were characterized using a JSM-6700F scanning electron microscopy (SEM), H-800 transmission electron microscope (TEM), and JEM-3010

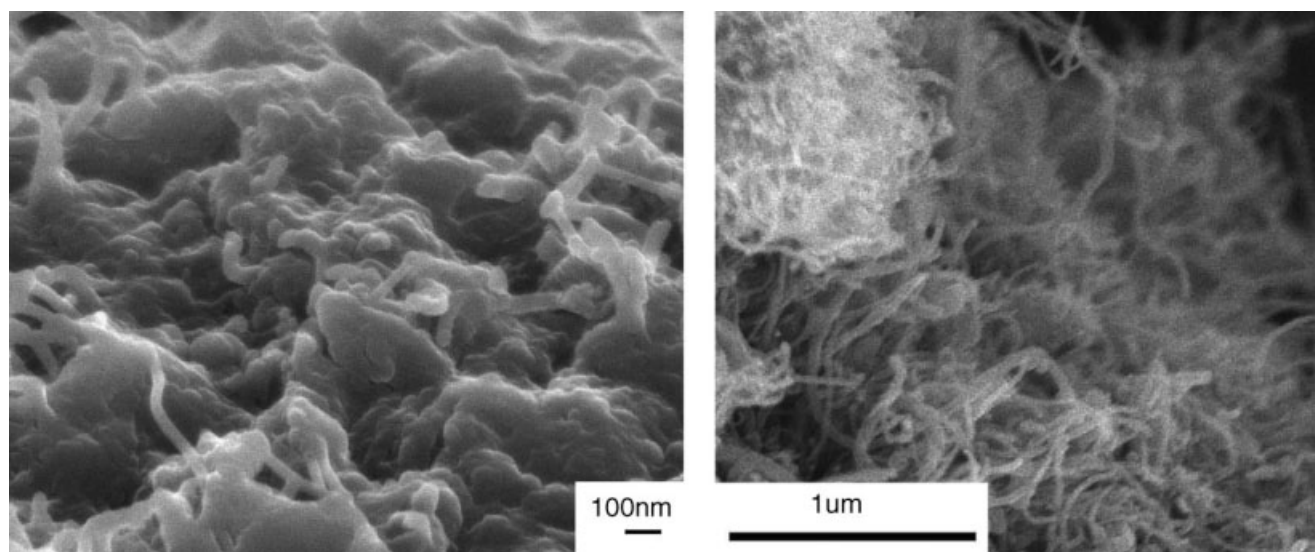


**Figure 2** SEM images of CNTs-MAH-PP composite and CNTs/PP composite.

high-resolution transmission electron microscope (HRTEM). An Instron model WDW-100 was used to perform the tensile tests on the composites, following the mounting specification indicated by GB1040-79 standard. The crosshead speed used was 10 mm/min. The electrical testing was performed on a ZC36 ultra-high resistance tester.

## RESULTS AND DISCUSSION

SEM and TEM are excellent techniques for investigating the morphology of composite. The distribution morphology of CNT in the sample is observed for PP-wrapped CNTs (CNTs-MAH-PP) composite and CNTs/PP, respectively (see Fig. 2). As Figure 2(a) shows, CNT is dispersed uniformly in the CNTs-MAH-PP composite, and there is no obvious aggregation of CNT in this sample. Furthermore, the

cylindrical CNT structure is embedded in the PP matrix. The diameter of tubes on the composite is about 60–80 nm, which is much thicker than that of pristine CNT. As a comparison, such uniform dispersion and wrapped structure are not found for the CNTs/PP composite in Figure 2(b). It is very different from that of CNTs-MAH-PP, and CNTs exist as entangled agglomerates. Therefore, it is useful to treat CNTs with MAH prior to compound with PP for improving the compatibility of CNTs with PP. The properties of CNTs-MAH-PP will benefit from the easily accomplished homogeneous dispersion of CNTs in the composite.

Figure 3 shows TEM and HRTEM morphology of the CNTs-MAH-PP composite. Apparently, PP could form a dense covering layer around the outer wall of CNT and CNTs are wrapped by thin PP layer as

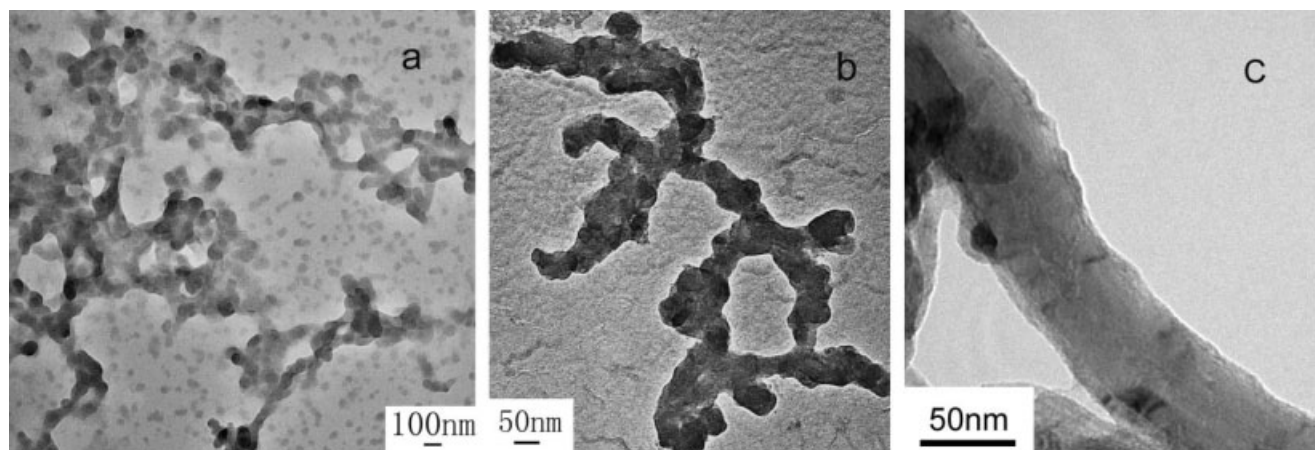


**Figure 3** TEM images of CNTs-MAH-PP composite.

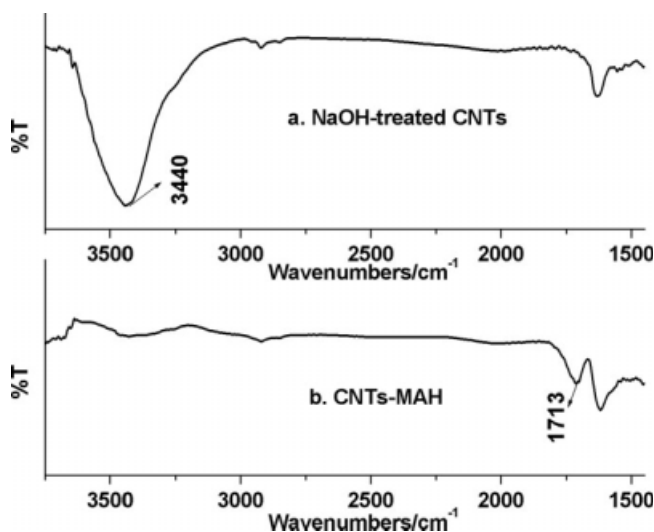


Figure 4 FTIR spectra of CNTs-OH and CNTs-MAH.

shown in Figure 3. By comparison with the diameter of the pristine nanotube (20–30 nm, not shown), the layer thickness is estimated to be 30–40 nm. These images reinforce the idea that there is a wrapping of the nanotubes by the surrounding polymer, which would lead to better nanotube–matrix interface and enhanced mechanical properties as a consequence of increased load transfer between the CNTs and PP. Figure 3(c) shows a high-resolution TEM image of a fully wrapped CNTs. It is clear that the CNTs have been fully and uniformly wrapped.

Figure 4 shows the IR spectra of CNTs-OH, without and with MAH treatment, respectively. In the spectrum of CNTs-OH without treatment with MAH [Fig. 4(a)], there was a strong peak at  $3440\text{ cm}^{-1}$ , which is assigned to the O–H stretches of hydroxyl group. After treatment with MAH, this peak disappeared, and a new peak at  $1713\text{ cm}^{-1}$  corresponding to C=O appeared in the CNTs-MAH spectrum [Fig. 4(b)]. These may be attributed to the ester reaction of hydroxyl groups in CNTs-OH with the anhydride functions in MAH. The MAH was attached on the surface of CNTs via ester bond. The attachment between CNTs and MAH was beneficial for the adhesion of PP with CNTs.

As Figure 5 shown, PP shows many absorption bands based on various vibrational modes in both spectra. Peaks at  $2800\text{--}3000\text{ cm}^{-1}$  region are attributed to C–H stretching vibrations. The  $1455\text{ cm}^{-1}$  peak is corresponding to asymmetric bend vibration of  $\text{CH}_3$ . Another peak at  $1373\text{ cm}^{-1}$  is assigned to the bend vibration of  $\text{CH}_3$  group of PP. For PP-wrapped CNTs [Fig. 5(b)], two new peaks at  $1716\text{ cm}^{-1}$  corresponding to C=O group and  $1633\text{ cm}^{-1}$  corresponding to C=C group were observed. The appearance of these two new peaks may be a signature to the grafting of MAH and PP. In addition, the

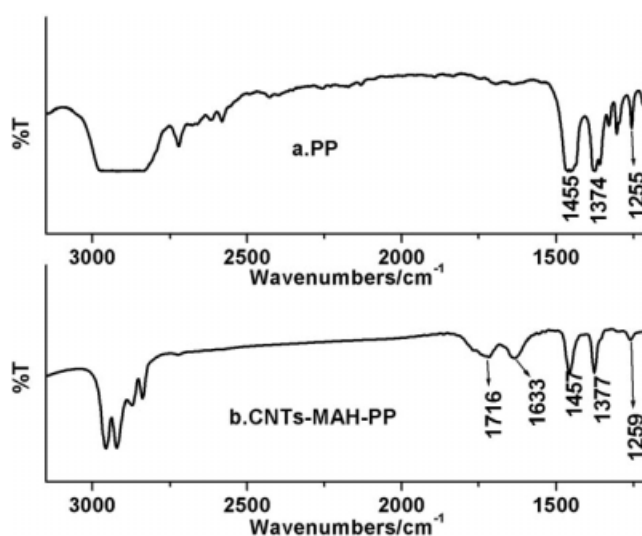


Figure 5 FTIR spectra of PP and CNTs-MAH-PP.

characteristic peaks of PP at  $1455$ ,  $1373$ ,  $1254$ , and  $1164\text{ cm}^{-1}$  in Figure 5(a) are found to be slightly shifted to  $1457$ ,  $1376$ ,  $1259$ , and  $1166\text{ cm}^{-1}$ , respectively. The high frequency shift about  $2\text{--}5\text{ cm}^{-1}$  is related to the covalent interactions of CNTs with PP via MAH.

We choose a typical CNTs-MAH-PP with 3 wt % CNTs as a representative and compare its mechanical and electrical properties with neat PP and CNTs/PP (contain 3 wt % CNTs) samples. The comparative results of tensile strength, Young's modulus, and volume resistivity tests are illustrated in Figures 6–10, respectively. All the reported results are the average of three measurements.

As shown in Figure 6, the tensile strength of CNTs-MAH-PP increased to 40 MPa, which is 110% higher than that for neat PP, and a 74% increase as compared to the CNTs/PP composite. For CNTs-

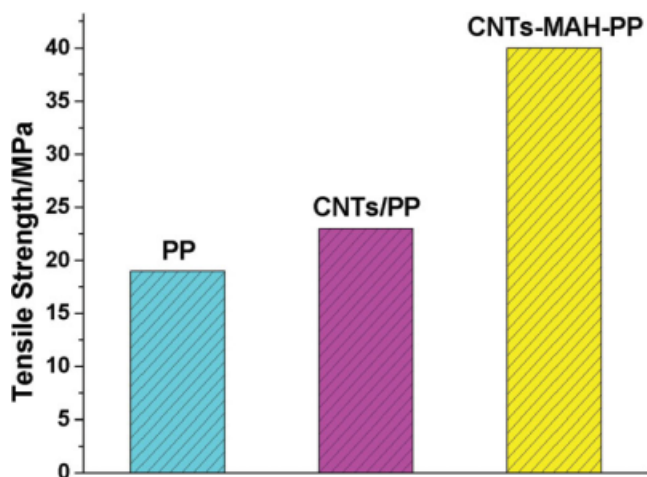
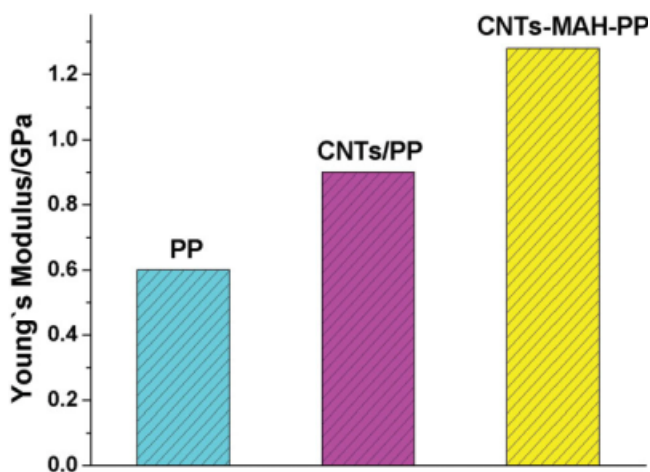


Figure 6 Tensile strength of neat PP, 3 wt % CNTs/PP, and 3 wt % CNTs-MAH-PP. [Color figure can be viewed in the online issue, which is available at [www.interscience.wiley.com](http://www.interscience.wiley.com).]



**Figure 7** Young's modulus of neat PP, 3 wt % CNTs/PP, and 3 wt % CNTs-MAH-PP. [Color figure can be viewed in the online issue, which is available at [www.interscience.wiley.com](http://www.interscience.wiley.com).]

MAH-PP with 3 wt % CNTs content, the Young's modulus (shown in Fig. 7) shows more than 113% improvement than neat PP. While at the same CNT content, the Young's modulus of CNTs/PP is also enhanced, but just 50% improvement in comparison to neat PP. The differences in mechanical property of PP reinforced with CNTs or with CNTs-MAH imply that the pretreatment of CNTs affects the ability of the spherulites to slip during tensile tests.<sup>22</sup> In contrast, PP reinforced with CNTs-MAH has a better mechanical property than reinforced with pristine CNTs. These should be attributed to the fact that CNTs without MAH treatment appear in the composite in the form of large agglomerates and cannot provide load-bearing capacity and load-transfer channel because of poor interfacial interaction. The poor interfacial interaction between CNTs and PP results in the slipping of spherulites during tensile tests. When PP is filled with CNTs-MAH, the situation is changed. The tensile strength and Young's modulus of the CNTs-MAH-PP are prominently increased owing to the improved stress transfer efficiency at the interface. For CNTs-MAH-PP composite, MAH acts as a "bridge" between PP and CNTs and helps to maintain a better load transfer from PP to the reinforcing CNTs, and the slippage of spherulites is effectively controlled. The significantly improvement of mechanical property of PP achieved indicates that the proposed covalent attachment of the CNTs to the PP was successful.

The tensile strength of the CNTs-MAH-PP composite with different CNTs content is shown in Figure 8. The addition of CNTs significantly increases the tensile strength. It is evident that even at a level of 2 wt % of CNTs blended in the PP, the tensile strength of the material can be effectively improved. This is a nearly 110% increase in tensile

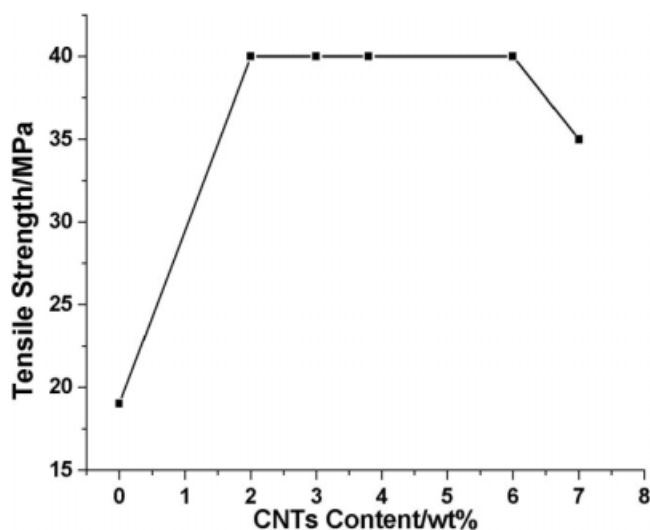


**Figure 8** Tensile strength of CNTs-MAH-PP at different CNT concentration.

strength of the PP at low addition level. On the other hand, the tensile strength of the CNTs-MAH-PP retains or slightly increases with the increase in CNT content. A decrease of the tensile strength is observed when the CNT content reaches 7 wt %. For high loading of nanotubes in the matrix, it becomes more difficult to produce well-dispersed CNTs in a composite. The CNTs tend to aggregate in bundles (due to van der Waals forces between CNTs), and the effective load transfer system is not easy to obtain as a consequence of poor interfacial interaction. As a conclusion, the CNT content in CNTs-MAH-PP composite should be controlled in 2–6 wt % to obtain the best reinforcement effect.

Figure 9 show the comparison results of volume electric resistivity obtained from neat PP, CNTs/PP

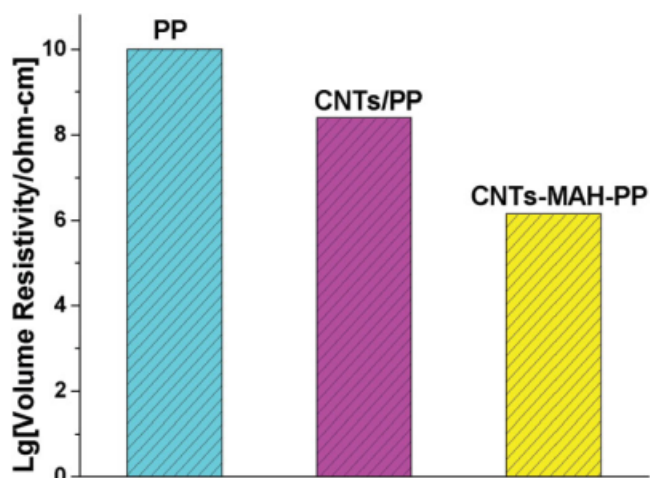


**Figure 9** Lg (volume resistivity) of neat PP, 3 wt % CNTs/PP, and 3 wt % CNTs-MAH-PP. [Color figure can be viewed in the online issue, which is available at [www.interscience.wiley.com](http://www.interscience.wiley.com).]

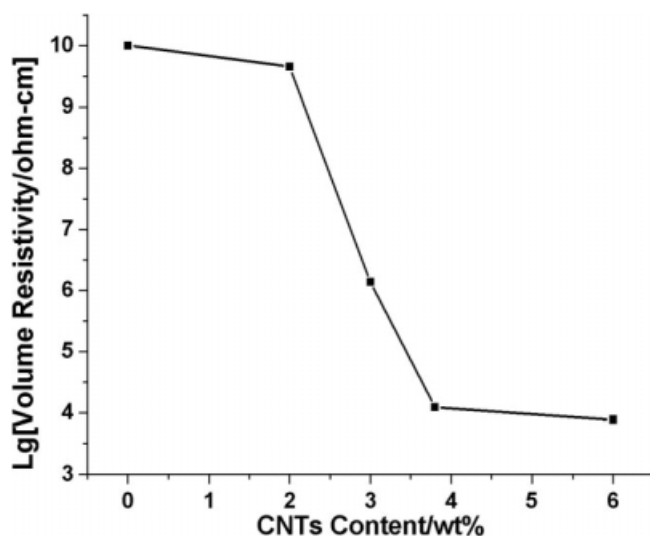


**Figure 10** Lg (volume resistivity) of CNTs-MAH-PP at different CNT concentrations.

(contain 3 wt % CNTs), and CNTs-MAH-PP (contain 3 wt % CNTs). It is found that the prominent decrease of volume resistivity is achieved with the incorporation of CNTs, while the volume resistivity of CNTs-MAH-PP decreases more quickly than that of CNTs/PP.

Figure 10 shows the effect of CNT content on volume resistivity of CNT-MAH-PP composite. At very low content of CNT, the resistivity gradually decreases with increasing nanotube content. However, at 4 wt %, a marked reduction in resistivity is observed. This stepwise change in resistivity is a result of the formation of an interconnected structure of CNTs and can be regarded as an electrical percolation threshold. This simply means that at contents between 2 and 4 wt % CNTs, a very high percentage of electrons are permitted to flow through the specimen due to the creation of an interconnecting conductive pathway.<sup>23,24</sup> At contents above 2 wt % CNT, the volume resistivity is decreased marginally with increase in CNT content. The volume resistivity of CNTs-MAH-PP is dramatically decreased by seven orders of magnitude with 4 wt % CNTs compared to neat PP. After that, with the increase in CNT content, the volume resistivity decreases little and almost retains the same magnitude. The dispersion of CNTs in PP became more difficult with the increase of CNT content. More and more CNTs exist as agglomerate and did not contribute to the volume resistivity. So the volume resistivity decreases little with the continuous increase of CNT content.

### CONCLUSIONS

In conclusion, we have fabricated CNTs-MAH-PP composites by *in situ* graft method. It is apparent that good dispersion of CNTs was obtained as dem-

onstrated by the SEM and TEM images. FTIR results indicated that covalent connect between CNTs and PP takes place. These strong covalent bonds benefit from the better interfacial adhesion between these immiscible matrix and hinder the CNTs to agglomerate. The tensile strength of PP-wrapped CNTs composite was 110% higher than that for neat PP, and a 74% increase as compared to the CNTs/PP (with the same CNTs content) composite. A strong mechanical behavior with up to 113% increase in Young's modulus of the neat PP was obtained. The electrical conductivity of PP-wrapped CNTs composite increased sharply by up to seven orders of magnitude with 4 wt % CNTs fillers because of the uniform dispersion of CNTs in the composite. Furthermore, the volume resistivity was decreased with increase in the CNT content that could be governed in a percolation-like power law with a relatively low percolation threshold.

### References

- Baughman, R. H.; Zakhidov, A. A.; de Heer, W. A. *Science* 2002, 297, 787.
- Thostenson, E. T.; Ren, Z. F.; Chou, T. W. *Compos Sci Technol* 2001, 61, 1899.
- Harris, P. J. F. *Inter Mat Rev* 2004, 49, 31.
- Breuer, O.; Sundararaj, U. *Polym Compos* 2004, 25, 630.
- Potschke, P.; Bhattacharyya, A. R.; Janke, A. *Carbon* 2004, 42, 965.
- Sandler, J. K. W.; Pegel, S.; Cadek, M.; Gojny, F.; Van, E. M.; Lohmar, J. *Polymer* 2004, 45, 2001.
- Seo, M. K.; Park, S. J. *Chem Phys Lett* 2004, 395, 44.
- Kashiwagi, T.; Grulke, E.; Hilding, J.; Harris, R.; Awad, W.; Douglas, J. *Macromol Rapid Commun* 2002, 23, 761.
- Zhang, D. W.; Shen, L.; Phang, I. Y.; Liu, T. *Macromolecules* 2004, 37, 256.
- Tang, W. Z.; Santare, M. H.; Advani, S. G. *Carbon* 2003, 41, 2779.
- Bhattacharyya, A. R.; Sreekumar, T. V.; Liu, T.; Kumar, S.; Ericson, L. M.; Hauge, R. H. *Polymer* 2003, 44, 2373.
- Cheah, K.; Simon, G. P.; Forsyth, M. *Polym Int* 2001, 50, 27.
- Shaffer, M. S. P.; Windle, A. H. *Adv Mater* 1999, 11, 937.
- Bin, Y.; Kitanaka, M.; Zhu, D.; Matsuo, M. *Macromolecules* 2003, 36, 6213.
- Ruan, S. L.; Gao, P.; Yang, X. G.; Yu, T. X. *Polymer* 2003, 44, 5643.
- Paiva, M. C.; Zhou, B.; Fernando, K. A. S.; Lin, Y.; Kennedy, J. M.; Sun, Y. P. *Carbon* 2004, 42, 2849.
- Curran, S. A.; Ajayan, P. M.; Blau, W. J. *Adv Mater* 1998, 10, 1091.
- O'Connell, M. J.; Bachilo, S. M.; Huffman, C. B.; Moore, V. C.; Strano, M. S.; Haroz, E. H.; Rialon, K. L.; Boul, P. J.; Noon, W. H.; Kittrell, C.; Ma, J. P.; Hauge, R. H.; Weisman, R. B.; Smalley, R. E. *Science* 2002, 297, 593.
- Tang, B. Z.; Xu, H. Y. *Macromolecules* 1999, 32, 2569.
- Chen, X. H.; Hu, J.; Li, W. H.; Liu, Y. Q.; Chen, C. S.; Wang, Y. G. *J Mater Sci Technol* 2008, 24, 279.
- Li, W. H.; Chen, X. H.; Zhang, G.; Chen, C. S.; Hu, J.; Xu, L. S.; Yang, Z. *Polym Mater Sci Eng* 2007, 23, 194.
- Shah, D.; Maiti, P.; Jiang, D. D.; Batt, C. A.; Giannelis, E. P. *Adv Mater* 2005, 17, 525.
- Park, S. J.; Kim, H. C.; Kim, H. Y. *J Colloid Interface Sci* 2002, 255, 145.
- Potschke, P.; Dudkin, S. M.; Alig, I. *Polymer* 2003, 44, 5023.